

Attempt to distinguish the origins of self-similarity by natural time analysis.

P. A. Varotsos,^{1,2} N. V. Sarlis,¹ E. S. Skordas,² H. K. Tanaka,³ and M. S. Lazaridou¹

¹Solid State Section, Physics Department, University of Athens,
Panepistimiopolis, Zografos 157 84, Athens, Greece

²Solid Earth Physics Institute, Physics Department,

University of Athens, Panepistimiopolis, Zografos 157 84, Athens, Greece

³Earthquake Prediction Research Center, Tokai University 3-20-1, Shimizu-cho, Shizuoka 424-8610, Japan

Self-similarity may originate from two origins, i.e., the process memory and the process' increments \in nite" variance. A distinction is attempted by employing the natural time . Concerning the first origin, we analyze recent data on Seismic Electric Signals, which support the view that they exhibit in nite"ly ranged temporal correlations. Concerning the second, slowly driven systems that emit bursts of various energies E obeying power-law distribution, i.e., $P(E) \sim E^{-\alpha}$, are studied. An interrelation between the exponent α and the variance σ^2 ($\langle h^2 \rangle - \langle h \rangle^2$) is obtained for the shuffled (randomized) data. In the latter, the most probable value of α is approximately equal to that of the original data. Finally, it is found that the differential entropy associated with the probability $P(\alpha)$ maximizes for α around 1.6 to 1.7, which is comparable to the value determined experimentally in diverse phenomena, e.g., solar flares, icequakes, dislocation glide in stressed single crystals of ice etc. It also agrees with the b-value in the Gutenberg-Richter law of earthquakes.

PACS numbers: 05.40.-a, 91.30.Dk, 05.45.Tp, 89.75.-k

I. INTRODUCTION

A large variety of natural systems exhibit irregular and complex behavior which at first looks erratic, but in fact possesses scale invariant structure (e.g., [1, 2]). A process $X(t)$ is called self-similar [3] if for some $H > 0$,

$$X(t) \stackrel{d}{=} H^H X(t/H) \quad H > 0; \quad (1)$$

where the symbol of equality refers here to all nite-dimensional distributions of the process on the left and the right, and the parameter H is called self-similarity index or exponent. Equation (1) means a \scale invariance" of the nite-dimensional distributions of $X(t)$, which does not imply, in stochastic processes, the same for the sample paths (e.g., [4]). Examples of self-similar processes are Brownian, fractional Brownian (fBm), Levy stable and fractional Levy stable motion (fLsm). Levy stable distributions (which are followed by many natural processes, e.g., [5, 6]) differ greatly from the Gaussian ones because they have heavy tails and their variance is in nite (e.g., [4, 7]).

An important point in analyzing data from natural systems that exhibit scale invariant structure, is the following: In several systems this nontrivial structure points to long-range temporal correlations; in other words, the self-similarity results from the process' memory only (e.g., the case of fBm). Alternatively, the self-similarity may solely result from the process' increments in nite variance, e.g., Levy stable motion. (Note, that in distributions that are applicable to a large variety of problems, extreme events have to be truncated for physical reasons, e.g., nite size

effects, when there is no in nity [8]—and this is why we write hereafter \in nite".) In general, however, the self-similarity may result from both these origins (e.g., fLsm). It is the main aim of this paper to discuss how a distinction of the two origins of self-similarity (i.e., process' memory, process' increments \in nite" variance) can be in principle achieved by employing the natural time analysis.

In a time series comprising N events, the natural time $\tau_k = k/N$ serves as an index [9, 10] for the occurrence of the k -th event. The evolution of the pair $(\tau_k; Q_k)$ is considered [9, 10, 11, 12, 13, 14, 15, 16, 17, 18, 19], where Q_k denotes in general a quantity proportional to the energy released in the k -th event. For example, for dichotomous signals Q_k stands for the duration of the k -th pulse while for the seismicity Q_k is proportional to the seismic energy released during the k -th earthquake [9, 17, 19] (which is proportional to the seismic moment M_0). The normalized power spectrum $\langle \tau \rangle$ was introduced [9, 10]:

$$\langle \tau \rangle = \frac{1}{N} \sum_{k=1}^N p_k \exp \left(-i \tau \frac{k}{N} \right)^2 \quad (2)$$

where $p_k = Q_k / \sum_{n=1}^N Q_n$ and $\tau = 2\pi$; stands for the natural frequency. When the system enters into the critical stage, the following relation holds [9, 10]:

$$\langle \tau \rangle = \frac{18}{5!^2} - \frac{6 \cos \tau}{5!^2} - \frac{12 \sin \tau}{5!^3}; \quad (3)$$

For $\tau \rightarrow 0$, Eq.(3) leads to [9, 10, 16] $\langle \tau \rangle \rightarrow 1/0.7!^2$ which reflects [17] that the variance of τ is given by $\sigma^2 = \langle \tau^2 \rangle - \langle \tau \rangle^2 = 0.7$, where $\langle \tau^2 \rangle = \sum_{k=1}^N p_k \tau_k^2$. It has been argued [17] that in the case of earthquakes, $\langle \tau \rangle$ for $\tau \rightarrow 0$, can be considered as an order param-

Electronic address: pvaro@otenet.gr

eter and the corresponding probability density distribution function (PDF) is designated by $P(\tau)$. Since, at $\tau = 0$, τ is linearly related to τ (because Eq.(2) leads to $\tau = 1 - 4^{-2} \tau$ for $\tau = 0$) one can study, instead of $P(\tau)$, the PDF of τ , i.e., $P(\tau)$. This will be used here. The entropy S in the natural time domain is defined as [9, 12] $S = -\sum p_k \ln p_k$, which depends on the sequential order of events [13, 14] and for infinitely ranged temporal correlations its value is smaller [12, 16] than the value $S_u (= 1/2 \ln 2 \approx 0.3466)$ of a "uniform" distribution (defined in Refs. [9, 11, 12, 13, 14], e.g. when all p_k are equal), i.e., $S < S_u$. The value of the entropy obtained [15] upon considering the time reversal T , i.e., $T p_k = p_{N-k+1}$, is labelled by S^* .

This paper is organized as follows: In Section II, we treat the case when the self-similarity solely results from the process' memory. Section III deals with the self-similarity resulting from the process' increments in finite variance by restricting ourselves to slowly driven systems that emit energy bursts obeying power law distributions. A brief discussion follows in Section IV, while Section V presents the main conclusion.

II. THE CASE OF TEMPORAL CORRELATIONS

We consider, as an example, Seismic Electric Signals (SES) activities which exhibit infinitely ranged temporal correlations [10, 11, 12]. Figure 1(a) shows a recent SES activity recorded at a station located in central Greece (close to Patras city, PAT) on February 13, 2006. It comprises 37 pulses, the durations Q_k of which vary between 1s and 40s (see Fig. 1(b)). The natural time representation of this SES activity can be seen in Fig. 1(b) and the computation of τ , S and S^* leads to the following values: $\tau = 0.072 \pm 0.002$, $S = 0.080 \pm 0.002$, $S^* = 0.078 \pm 0.002$. These values obey the conditions $\tau < 0.070$ and $S; S^* < S_u$ that have already been found [10, 12, 18] to be obeyed for other SES activities. If we repeat the computation for surrogate data obtained by shuffling the durations Q randomly (and hence their distribution is conserved), the corresponding quantities, designated by adding a subscript "shuf", have the following values: $\tau_{shuf} = 0.082$ and $S_{shuf} (= S^*_{shuf}) = 0.091$ with standard deviations 0.008 and 0.011 respectively. They are almost equal to the corresponding values of a "uniform" distribution, i.e., $\tau_u = 0.0833$ and $S_u = 0.0966$, although the experimental error in this case is large due to the small number of pulses. By applying the same procedure to other SES activities reported earlier [15], we find (see Table I) that actually $\tau_{shuf} \approx \tau_u$ and $S_{shuf} \approx S_u$. This points to the conclusion that the self-similarity of SES activity results from the process' memory only, which agrees with an independent analysis of Ref. [4].

In addition, the Detrended Fluctuation Analysis (DFA) [20, 21] in natural time of the SES activity de-

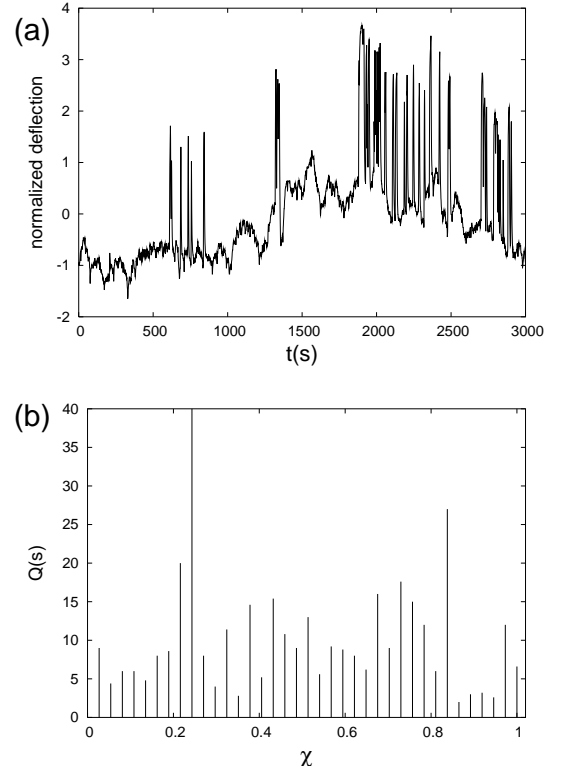


FIG. 1: (a) An SES activity recently recorded at PAT station (sampling rate $f_{exp} = 1\text{ Hz}$). The actual electric field E is 6 mV/km , but here the signal is presented in normalized units, i.e., by subtracting the mean value and dividing by the standard deviation. (b) How the SES activity in (a) is read in natural time.

icted in Fig. 1, leads to an exponent $D_{DFA} = 1.07 \pm 0.36$, which agrees with the earlier finding $D_{DFA} \approx 1$ in several other SES activities [11]. Interestingly, the values of the quantities $\tau; S; S^*$ and D_{DFA} are consistent with the results deduced from a numerical simulation in IBM time series described in Ref. [18]; the latter showed that when $D_{DFA} \approx 1$ the corresponding values are: $\tau \approx 0.070$, $S \approx S^* \approx 0.080$. Figure 2 depicts the most probable value τ_p of τ versus D_{DFA} resulting from such a numerical simulation.

III. THE CASE OF POWER LAW DISTRIBUTIONS

We now study a case of self-similarity resulting from the process' increments in finite variance. Here, we restrict ourselves to slowly driven systems that emit energy bursts obeying power law distribution

$$P(E) \sim E^{-\alpha} \quad (4)$$

where α is constant. In a large variety of such systems, in diverse fields, an inspection of the recent experimental data reveals that the exponent lies in a narrow range,

TABLE I: The values of γ , γ_{shuf} , S , S and S_{shuf} for the SES activities mentioned in Ref.[15] as well as the one (PAT) depicted in Fig.1. The numbers in parentheses denote the standard deviation for the distributions of γ_{shuf} and S_{shuf} in the shuffled data.

Signal	γ	γ_{shuf}	S	S	S_{shuf}^b
K1	0.063 0.003 ^a	0.083 (0.005)	0.067 0.003 ^a	0.074 0.003 ^a	0.096 (0.007)
K2	0.078 0.004 ^a	0.082 (0.007)	0.081 0.003 ^a	0.103 0.003 ^a	0.094 (0.009)
A	0.068 0.004 ^a	0.082 (0.007)	0.070 0.008 ^a	0.084 0.008 ^a	0.092 (0.010)
U	0.071 0.004 ^a	0.082 (0.009)	0.092 0.004 ^a	0.071 0.004 ^a	0.093 (0.012)
T1	0.084 0.007 ^a	0.082 (0.007)	0.088 0.007 ^a	0.098 0.010 ^a	0.091 (0.010)
C1	0.074 0.002 ^a	0.082 (0.008)	0.083 0.004 ^a	0.080 0.004 ^a	0.092 (0.011)
P1	0.075 0.004 ^a	0.082 (0.008)	0.087 0.004 ^a	0.081 0.004 ^a	0.090 (0.011)
P2	0.071 0.005 ^a	0.082 (0.009)	0.088 0.003 ^a	0.072 0.015 ^a	0.091 (0.012)
E1	0.077 0.017 ^a	0.083 (0.008)	0.087 0.007 ^a	0.081 0.007 ^a	0.092 (0.010)
PAT	0.072 0.002	0.082 (0.008)	0.080 0.002	0.078 0.002	0.091 (0.011)

^afrom Ref.[15]

^bnote that $S_{shuf} = S_{shuf}$ as mentioned in the text.

TABLE II: Compilation of the experimental values of the power-law exponent determined in different processes.

Process / type of measurement	γ	References
Dislocation glide in hexagonal ice single crystals (Acoustic emission)	1.6	[23]
Solar flares	1.5 – 2.1	[24, 33, 34, 35]
Microfractures before the breakup of wood (acoustic emission)	1.51	[36, 37]
Microfractures before the breakup of fiberglass (acoustic emission)	2.0	[36, 37]
Earthquakes	1.5 – 1.8 ($\beta = 0.8$ to 1.2)	See Ref.[27] and references therein
Icequakes	1.8 ($\beta = 1.25$)	See p.212 of [38] and references therein

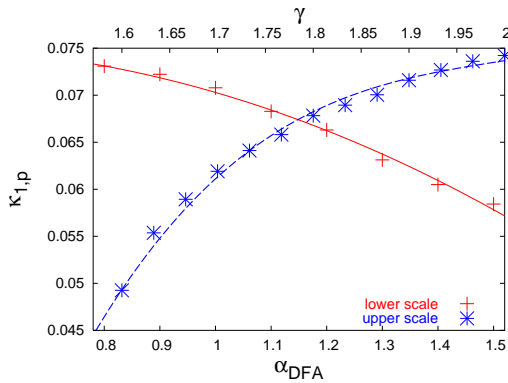


FIG. 2: (Color online) The values of $\kappa_{1,p}$ as a function of α_{DFA} for the case of the fBm simulations of Ref.[18] (crosses, lower scale) or as a function of γ for power law distributed data (asterisks, upper scale). They have been estimated by following the procedure described in the Appendix B of Ref.[17]. The corresponding lines have been drawn as a guide to the eye.

ie., 1:5 – 2:1 (and mostly even within narrower bounds, ie., $\gamma = 1.5$ to 1.8). To realize the diversity of the phenomena that exhibit the aforementioned property, we compile some indicative examples in Table II, which are the following.

First, crystalline materials subjected to an external stress, display bursts of activity owing the nucleation and motion of dislocations. These sudden local changes produce acoustic emission waves which reveal that a large number of dislocations move cooperatively in an intermittent fashion (e.g., see [22] and references therein). As a precise example, we include in Table II the results of acoustic emission experiments on stressed single crystals of ice under viscoelastic deformation (creep), which show that the probability distribution of energy bursts intensities obey a power-law distribution with $\gamma = 1.6$ spanning many decades (see Fig.1 of [23]). Second, we consider the case of solar flares that represent impulsive energy releases in the solar corona (e.g. see Ref. [24] and references therein; see also Ref.[25] in which it is concluded

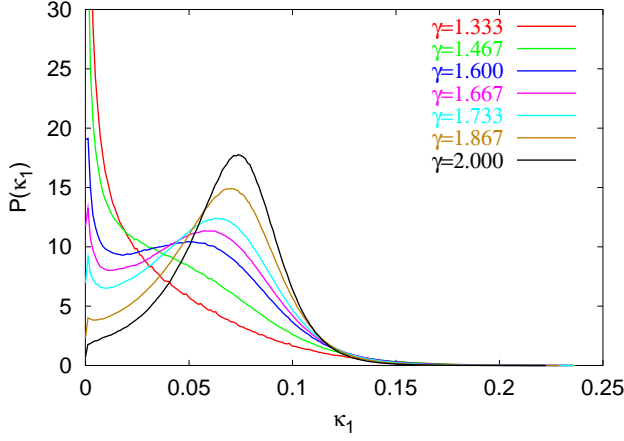


FIG. 3: (Color online) The probability density function $P(\kappa_1)$ versus κ_1 for several values of γ (see the text and [29]).

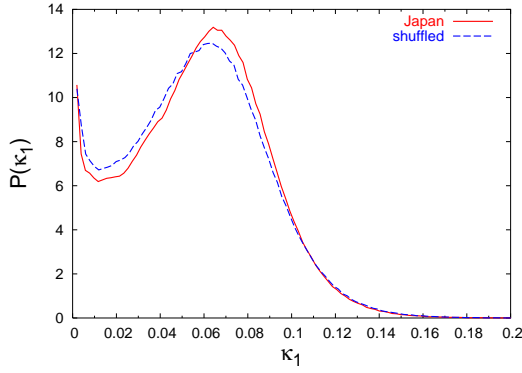


FIG. 4: (Color online) The PDFs of κ_1 when using either the actual seismic catalogue of Japan (solid) treated in Ref.[17] or the same data in random order (dashed).

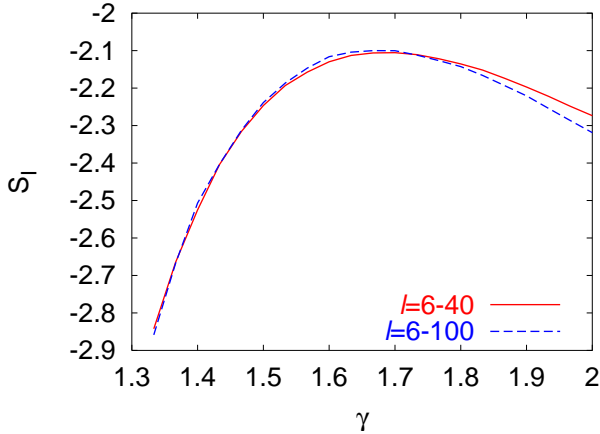


FIG. 5: (Color online) The calculated values of the differential entropy S_1 versus the exponent γ . Two window lengths are used and their results are almost the same.

that earthquakes and solar flares exhibit the same distributions of sizes, interoccurrence times, and the same temporal clustering). This energy release is observed in various forms: thermal, soft and hard x-ray emissions, accelerated particles etc. The statistical analysis of these impulsive events show that the energy distribution exhibit, over several orders of magnitude, a power-law with exponents ranging from 1.5 to approximately 2.1 (depending on the experimental procedure and the geometrical assumptions adopted in the analysis). Other examples are: acoustic emission from microfractures before the breakup of heterogeneous materials (wood, fiberglass), icequakes and earthquakes.

Concerning the latter, the best known scaling relation is the Gutenberg-Richter law [26], which states that the (cumulative) number of earthquakes with magnitude greater than m occurring in a specified area and time is given by

$$N(>m) = 10^{b-m} \quad (5)$$

where b is a constant, which varies only slightly from region to region (cf. Eq.(5) holds both regionally and globally) being generally in the range $0.8 \leq b \leq 1.2$ (see [27] and references therein). Considering that the seismic energy E released during an earthquake is related [28] to the magnitude through $E = 10^{1.5m}$ where c is around 1.5—Eq.(5) turns to Eq.(4), where $\gamma = 1 + b = 1.5$. Hence, $b = 1$ means that the exponent is around $\gamma = 1.6$ to 1.7 .

The following procedure is now applied: We generate (see also [29]) a large amount of artificial data obeying Eq.(5) for a certain γ value. These randomized ("shuffled" [13]) data are subsequently analyzed, in the natural time domain, for each γ value, with the following procedure [17]: First, calculation of the variance κ_1 is made for an event taking time windows for 6 to 40 consecutive events (the choice of the precise value of the upper limit is not found decisive, because practically the same results are obtained even if the number of consecutive events was changed from 6–40 to 6–100, as it will be further discussed below). And second, this process was performed for all the events by scanning the whole dataset. In Fig.3 we plot the quantity $P(\kappa_1)$ versus κ_1 for several γ -values. The most probable value κ_{1p} (for $\gamma = \text{constant}$) is also plotted in Fig.2 versus the corresponding γ -value. This curve interrelates κ_1 and γ for the shuffled data (thus an eventual process' memory is here destroyed [13]) and hence the plotted κ_{1p} values (which differ markedly from κ_u) correspond to the self-similarity resulting from the heavy-tailed distribution only.

In order to identify the origin of self-similarity in a real data set, let us consider here the example of earthquakes. Using the Japan catalogue mentioned in Ref.[17], we give in Fig.4 the two curves $P(\kappa_1)$ versus κ_1 that result when the aforementioned calculation is made by means of a window of 6–40 consecutive events sliding through either the original catalogue or a shuffled one. Comparing the resulting κ_{1p} values (both of which differ from κ_u) we see that the value of the surrogate data ($\kappa_{1p} = 0.064$)

differs slightly from the one (≈ 0.066) corresponding to the original data. This reflects that the self-similarity mainly originates from the process' increments \in nite" variance. Note, however, that the $\sigma_{1,p}$ value of the original data is comparable to the value $\sigma_1 = 0.070$ that was found in infinitely ranged temporal correlations. This merits further investigation.

IV. DISCUSSION

Here, we discuss a challenging point that emerges from a further elaboration of the results depicted in Fig. 3. First, note that upon increasing the σ value from $\sigma = 1.3$ to 2.0 , the feature of the curve changes significantly, becoming bimodal at intermediate σ -values. Second, we calculate, for each σ -value studied, the so called differential entropy, defined as $S_I = -\int P(\sigma) \ln P(\sigma) d\sigma$, which is the Shannon information entropy of a continuous probability distribution, e.g., see [30]. (Note that, the Shannon information entropy is static entropy and not a dynamic one [13].) Finally, we investigate the resulting S_I -values versus σ . Such a plot is given in Fig. 5, whose inspection reveals that S_I maximizes at a value of σ lying between $\sigma = 1.6$ and $\sigma = 1.7$, which is more or less comparable with the experimental values, see Table II. (This value is not practically affected by the window length (l) chosen; in reality, upon increasing l from $l = 10$ to $l = 1000$, we find that, σ -value at which S_I maximizes in Fig. 2, decreases only slightly from $\sigma = 1.70$ to $\sigma = 1.63$.) In particular for the case of earthquakes this σ -value corresponds to $b \approx 1$, thus agreeing with the experimental findings mentioned above. Does it mean that the b or σ value

can be determined just by applying the Maximum Entropy Principle in the sense developed by Jaynes [31, 32], who suggested to look at statistical mechanics as a form of statistical inference and start statistical physics from the principle of maximum entropy inference (MaxEnt)? This is not yet clear, because a widely accepted formalism for non-equilibrium statistical mechanics is still lacking.

Finally, the fact that in some experiments the resulting σ -values differ slightly from $\sigma = 1.6$ to 1.7 predicted from Fig. 5 could be attributed to the following: Figure 5 is based on randomized data, while the actual data may also exhibit temporal correlations (e.g., the case of after-shocks). In addition, finite size effects [8] might play a significant role.

V. CONCLUSION

In summary, the origin of self-similarity may be distinguished as follows: If self-similarity exclusively results from the process' memory, the σ_1 value should change to $\sigma_u = 0.0833$ (and the values of S_I to $S_u = 0.0966$) for the surrogate data. On the other hand, if the self-similarity results from process' increments \in nite" variance only, the $\sigma_{1,p}$ values should be the same (but differing from σ_u) for the original and surrogate data.

When studying the differential entropy associated with the PDF of σ_1 it maximizes when the exponent σ lies in the narrow range 1.6 to 1.7 , in agreement with the experimental findings in diverse fields. This, for the case of earthquakes, immediately reflects that the b -value in the Gutenberg-Richter law is $b \approx 1$, as actually observed.

-
- [1] C.-K. Peng, S. Havlin, and H. E. Stanley, *Chaos* 5, 82 (1995).
 - [2] T. Kalisky, Y. Ashkenazy, and S. Havlin, *Phys. Rev. E* 72, 011913 (2005).
 - [3] J. W. Lamperti, *Trans. Am. Math. Soc.* 104, 62 (1962).
 - [4] A. Weron, K. Burnecki, S. Mercik, and K. Weron, *Phys. Rev. E* 71, 016113 (2005).
 - [5] C. Tsallis, S. V. F. Levy, A. Souza, and R. Maynard, *Phys. Rev. Lett.* 75, 3589 (1995).
 - [6] C. Tsallis, S. V. F. Levy, A. Souza, and R. Maynard, *Phys. Rev. Lett.* 77, 5442 (1996).
 - [7] N. Scaletta and B. J. West (2005), *physics/0509249*.
 - [8] M. Ausloos and R. Lambiotte, *Phys. Rev. E* 73, 011105 (2006).
 - [9] P. A. Varotsos, N. V. Sarlis, and E. S. Skordas, *Practica of Athens Academy* 76, 294 (2001).
 - [10] P. A. Varotsos, N. V. Sarlis, and E. S. Skordas, *Phys. Rev. E* 66, 011902 (2002).
 - [11] P. A. Varotsos, N. V. Sarlis, and E. S. Skordas, *Phys. Rev. E* 67, 021109 (2003).
 - [12] P. A. Varotsos, N. V. Sarlis, and E. S. Skordas, *Phys. Rev. E* 68, 031106 (2003).
 - [13] P. A. Varotsos, N. V. Sarlis, E. S. Skordas, and M. S. Lazaridou, *Phys. Rev. E* 70, 011106 (2004).
 - [14] P. A. Varotsos, N. V. Sarlis, E. S. Skordas, and M. S. Lazaridou, *Phys. Rev. E* 71, 011110 (2005).
 - [15] P. A. Varotsos, N. V. Sarlis, H. K. Tanaka, and E. S. Skordas, *Phys. Rev. E* 71, 032102 (2005).
 - [16] P. Varotsos, *The Physics of Seismic Electric Signals (TERRAPUB, Tokyo, 2005)*.
 - [17] P. A. Varotsos, N. V. Sarlis, H. Tanaka, and E. S. Skordas, *Phys. Rev. E* 72, 041103 (2005).
 - [18] P. A. Varotsos, N. V. Sarlis, E. S. Skordas, H. Tanaka, and M. S. Lazaridou, *Phys. Rev. E* 73, (in press) (2006).
 - [19] H. Tanaka, P. A. Varotsos, N. V. Sarlis, and E. S. Skordas, *Proc. Japan Acad. Ser. B* 80, 283 (2004).
 - [20] C.-K. Peng, S. V. Buldyrev, S. Havlin, M. Simons, H. E. Stanley, and A. L. Goldberger, *Phys. Rev. E* 49, 1685 (1994).
 - [21] S. V. Buldyrev, A. L. Goldberger, S. Havlin, R. N. Mantegna, M. E. M. M. Atsa, C.-K. Peng, M. Simons, and H. E. Stanley, *Phys. Rev. E* 51, 5084 (1995).
 - [22] M. Koslowski, R. O. LeSar, and R. Thomson, *Phys. Rev. Lett* 93, 125502 (2004).
 - [23] M. C. Miguel, A. Vespignani, S. Zapperi, J. Weiss, and J. R. Gras, *Nature (London)* 410, 667 (2001).

- [24] G. Nigro, F. Malara, V. Carbone, and P. Veltri, *Phys. Rev. Lett.* 92, 194501 (2004).
- [25] L. de Arcangelis, C. Godano, E. Lippiello, and M. Nicodemi, *Phys. Rev. Lett.* 96, 051102 (2006).
- [26] B. Gutenberg and C. F. Richter, *Seismicity of the Earth and Associated Phenomena* (Princeton Univ. Press, Princeton, New York, 1954).
- [27] J. B. Rundle, D. L. Turcotte, R. Shcherbakov, W. Klein, and C. Sammis, *Reviews of Geophysics* 41, 1019 (2003).
- [28] H. Kanamori, *Nature (London)* 271, 411 (1978).
- [29] For the case of earthquakes, the curves of Fig. 3 can be obtained as follows: We first generate, for each b -value, artificial data above a certain magnitude threshold (e.g., $m = 0$) that obey the Gutenberg-Richter relation $N(>m) = 10^{bm}$. This is repeated for various b -values by keeping the total number ($5 \cdot 10^5$) of events constant (which implies that when changing the b -value, the maximum magnitude m_{\max} involved in the calculation also changes). These data are subsequently shuffled and analyzed in natural time, for each b -value, with the procedure described in the text as well as in P. Varotsos et al., *Proc. Jap. Acad. Ser. B* 80, 429 (2004).
- [30] R. Garbaczewski (2004), [quant-ph/0408192](https://arxiv.org/abs/quant-ph/0408192).
- [31] E. T. Jaynes, *Phys. Rev.* 106, 620 (1957).
- [32] E. T. Jaynes, *Probability Theory: The Logic of Science* (Cambridge Univ. Press, New York, 2003).
- [33] M. J. Aschwanden and et al., *Astrophys. J.* 535, 1047 (2000).
- [34] E. N. Pamell and P. E. Jupp, *Astrophys. J.* 529, 554 (2000).
- [35] D. Hughes, M. Paczuski, R. O. Dendy, P. Helander, and K. G. McClements, *Phys. Rev. Lett.* 90, 131101 (2003).
- [36] A. Garcimartín, A. Guarino, L. Bellon, and S. Giliberto, *Phys. Rev. Lett.* 79, 3202 (1997).
- [37] A. Guarino, S. Giliberto, A. Garcimartín, M. Zei, and R. Scorzetti, *Eur. Phys. J. B* 26, 141 (2002).
- [38] J. Weiss, *Surveys in Geophysics* 24, 185 (2003).